

Properties of the Radio-Emitting Gas Around SgrA*

Abraham Loeb^{1,2} & Eli Waxman³

¹ *Astronomy Department, Harvard University, 60 Garden Street, Cambridge, MA 02138, USA*

² *Einstein Minerva center, Weizmann Institute of Science, Rehovot 76100, Israel, and*

³ *Physics Faculty, Weizmann Institute of Science, Rehovot 76 100, Israel*

We show that the radial profiles of the temperature and density of the electrons as well as the magnetic field strength around the massive black hole at the Galactic center, Sgr A*, may be constrained directly from existing radio data without any need to make prior assumptions about the dynamics of the emitting gas. The observed spectrum and wavelength-dependent angular size of Sgr A* indicate that the synchrotron emission originates from an optically-thick plasma of quasi-thermal electrons. We find that the electron temperature rises above the virial temperature within tens of Schwarzschild radii from the black hole, suggesting that the emitting plasma may be outflowing. Constraints on the electron density profile are derived from polarization measurements. Our best-fit results differ from expectations based on existing theoretical models. However, these models cannot be ruled out as of yet due to uncertainties in the source size measurements. Our constraints could tighten considerably with future improvements in the size determination and simultaneous polarization measurements at multiple wavelengths.

I. INTRODUCTION

The supermassive black hole at the Galactic center, Sgr A*, occupies the largest angle on the sky among all known black holes. Its extended image provides an excellent opportunity to study the physics of low-luminosity accretion flows.

The bolometric luminosity of Sgr A* $\sim 10^{36}$ erg s $^{-1}$ is ~ 8.5 orders of magnitude smaller than the Eddington limit for its black hole mass of $\sim 4 \times 10^6 M_\odot$. Over the past decade various theoretical models have been proposed to explain the low luminosity of Sgr A* despite the large gas reservoir from stellar winds in its vicinity. Among the early models invoked was an *Advection Dominated Accretion Flow (ADAF)* involving hot protons and cold electrons with a low radiative efficiency at the Bondi accretion rate of $\sim 10^{-5} M_\odot$ yr $^{-1}$ [21]. Subsequently, the detection of linear polarization was used to set an upper limit on the electron density near the black hole, which ruled out the original ADAF proposal [1, 17, 22] and favored shallower density profiles with a lower accretion rate such as in a *Convection Dominated Accretion Flow (CDAF)* [23]. Later variants of the ADAF model allowed for outflows, namely mass loss from the inflowing gas [2]. Most recently, an improved *Radiatively Inefficient Accretion Flow (RIAF)* model was proposed, involving substantial mass loss (although the outflowing mass is ignored in calculating the radio emission), a non-thermal component of electrons, and different electron and proton temperatures. Other models associated the radio emission with a jet [30] or a compact torus near the black hole [15].

In parallel to these modelling developments, the data on Sgr A* has improved dramatically over the past few years. The latest observations include new determinations of the size, spectral luminosity, polarization and rotation measure of the source as a function of wave-

length [14, 18, 27, 29]. With the rich data set that is now available, it is timely to remove any theoretical prejudice and ask: *what does the data alone tell us about the properties of the radiating gas?* In addressing this minimal question here, we deviate from past practice of modelers who made assumptions about the dynamics of the accreting gas before interpreting the observational data on Sgr A*. We avoid dynamical assumptions and attempt to constrain the properties of the radio-emitting gas directly from the data itself.

As discussed in detail in § II below, the measurements of the source size at different radio wavelengths provide crucial constraints on the properties of the gas surrounding Sgr A*. Current size measurements are unfortunately subject to large error bars, which in turn imply large uncertainties in the inferred gas properties. Our analysis provides an estimate of the spatial dependence of gas properties based on current measurements, adopting a frequency dependent size $r \propto \nu^\alpha$ with $\alpha = 1 \pm 0.3$ [14, 27]. Our methodology demonstrates how more accurate measurements may be used to obtain better constraints with no model-dependent assumptions about the dynamics of the gas.

In the different subsections of § II we apply our approach to various aspects of the data on Sgr A* that are currently available. We compare our results to previous work in § III. Finally, § IV summarizes our main conclusions.

II. EMPIRICAL CONSTRAINTS

II.1. Radio Spectrum and Size: Data

The spectral luminosity of SgrA* is time dependent. As illustrated in Fig. 1, the observed specific luminosity L_ν per unit frequency ν at the brighter emission epochs

[8, 34] is well described by a power-law form in the frequency range of 3–1000 GHz,

$$\nu L_\nu = 1.7 \times 10^{34} \nu_{11}^{1.4} \text{ erg s}^{-1} \quad (1)$$

where $\nu_{11} \equiv (\nu/10^{11} \text{ Hz})$. Since the flux measured at the times used for size determination is close to the brighter emission values, we will use this power-law index in our phenomenological discussion.

We note that at low frequencies $< 3 \text{ GHz}$ the observed flux somewhat exceeds the flux given by Eq. (1) [equivalently, fitting a power-law only to the data at $< 10 \text{ GHz}$ would result in a fit that under-predicts the flux at higher frequencies (as indicated by the dashed line in Fig. 1), i.e. in a "sub-mm excess"]. This deviation is of no significance to the analysis below, which focuses on higher frequencies, $> 10 \text{ GHz}$. It does imply, however, that in applying our simple analytic results to the lowest observed frequencies, some minor quantitative modifications would need to be introduced. As explained below, we argue that the radio flux is dominated at different frequencies by plasma located at different radii. The deviation from Eq. (1) below 3 GHz implies therefore that the gas temperature and magnetic field strength at large radii, $\gtrsim 10^{14.5} \text{ cm}$, differ slightly from those obtained using our simple power-law scalings, which are based on Eq. (1).

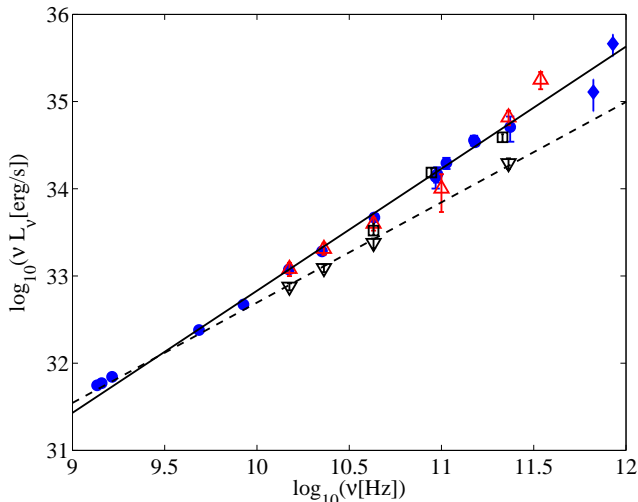


FIG. 1: Specific luminosity of Sgr A* from simultaneous multi-frequency data of Falcke et al. [8, filled circles], and Zhao et al. [34, up/down triangles representing the flux at different times, close to the times of maximum/minimum in the 1 mm flux]. Diamonds denote flux measurements by Zylka et al. [35, 666 GHz] and Serabyn et al. [25, 850 GHz]. Squares denote the flux densities derived from the data used for size determination, given in Krichbaum et al. [13, 14] (for 1.4 mm and 3.4 mm) and in Shen et al. [27] (for 7 mm). The solid line shows the power-law relation $\nu L_\nu = 1.7 \times 10^{34} \nu_{11}^{1.4} \text{ erg s}^{-1}$, and the dashed line is $0.7 \times 10^{34} \nu_{11}^{1.2} \text{ erg s}^{-1}$. The assumed distance to Sgr A* is 8 kpc.

As demonstrated in § II.2 below, measurements of the size of Sgr A* at various radio wavelengths provide important constraints on the emitting gas [5, 14, 27]. For a black hole mass of $M = 4 \times 10^6 M_\odot$ [7], the radial scale is set by the Schwarzschild radius of $R_s = 1.2 \times 10^{12} \text{ cm}$, which corresponds to an angle of 0.01 mas on the sky at our adopted distance of 8 kpc. Table I presents the latest data from Krichbaum et al. [14] and compares the inferred brightness temperature T_b to the virial temperature [36]. The brightness temperature [37] at a radius r from Sgr A* where the emissivity at an observed frequency ν peaks, is defined through the relation

$$\nu L_\nu = 4\pi r^2(\nu) \times f_g \times \frac{2\nu^3}{c^2} T_b(\nu), \quad (2)$$

where the geometric coefficient $f_g \leq 1$ is the ratio between the emission surface area and the area of a sphere of radius r ($f_g = 1$ for a sphere and $f_g = 0.5$ for a two-sided disk with the same radius). We conservatively assume that the surface area scales as r^2 since this provides the lowest brightness temperature (which, as we will show, is already above the virial temperature at large radii). We define the virial temperature T_v by equating the thermal kinetic energy of the plasma to half of the gravitational potential energy per proton,

$$2 \times \frac{3}{2} T_v = \frac{GMm_p}{2r}, \quad (3)$$

where m_p is the proton mass. (Note that the "escape temperature" at which the thermal kinetic energy of the plasma exceeds its gravitational potential energy is $2T_v$.) Using Eq. (1) and $M = 4 \times 10^6 M_\odot$ we obtain

$$T_b = 7.6(2f_g)^{-1} \nu_{11}^{-1.6} r_{13}^{-2} \text{ MeV}, \quad (4)$$

$$T_v = 9.5 r_{13}^{-1} \text{ MeV}, \quad (5)$$

where $r_{13} \equiv (r/10^{13} \text{ cm})$. Table I shows that T_b must be close to T_v at $r_{13} = 1$, and that there is preliminary evidence that T_b/T_v increases with radius.

Shen et al. [27] infer a power-law dependence of the intrinsic size of Sgr A* on wavelength λ of $r \propto \lambda^\beta$, with $\beta = 1.09 \pm 0.33$. For our phenomenological analysis we use

$$r_{13} = 1.0 \nu_{11}^{-1/\alpha}, \quad \nu_{11} = 1.0 r_{13}^{-\alpha} \quad (6)$$

with $\alpha \equiv \beta^{-1} \approx 1 \pm 0.3$, implying

$$2f_g \frac{T_b}{T_v} = 0.8 r_{13}^{1.6\alpha-1}. \quad (7)$$

II.2. Radio Spectrum and Size: Implications

The observed radio luminosity originates most likely from synchrotron emission by relativistic electrons [12].

TABLE I: Measured size and brightness temperature of Sgr A*. The listed radii are related to the FWHM intrinsic sizes of Krichbaum et al. [14] by $r = 0.5 \times \text{FWHM}/0.76$ (see footnote [36]).

λ [mm]	ν_{11}	r_{13}	$2f_g T_b$ [MeV]	T_v [MeV]	$2f_g T_b/T_v$
1.4	2.1	0.86 ± 0.47	$2.4^{+9}_{-1.4}$	11	$0.2^{+0.2}_{-0.08}$
3.4	0.88	1.2 ± 0.23	$7.2^{+4}_{-2.2}$	8.0	$0.8^{+0.2}_{-0.14}$
7	0.43	2.0 ± 0.55	$4.8^{+4.4}_{-1.8}$	4.8	$1.0^{+0.4}_{-0.2}$

The frequency dependence of source size implies that the emission cannot originate from an optically-thin plasma. To see this, consider the electrons at r dominating the emission at a frequency $\nu(r)$. If the optical depth is small, then these electrons would produce a spectrum $\nu L_\nu \propto \nu^{4/3}$ at $\nu < \nu(r)$, close to the observed spectrum at these frequencies. This implies that the emission at $\nu < \nu(r)$ would be dominated by electrons at r , which is inconsistent with the frequency dependence of source size. We therefore conclude that the optical depth for synchrotron self-absorption satisfies $\tau_\nu[\nu(r), r] \geq 1$. For a similar reason, the characteristic synchrotron emission frequency $\nu_c(r) = \langle \gamma_e^2 \rangle (eB/2\pi m_e c)$ of the electrons at r [dominating the emission at a frequency $\nu(r)$] must satisfy $\nu_c(r) \approx \nu(r)$. If $\nu_c(r) \gg \nu(r)$ then for $\tau_\nu[\nu(r), r] \gg 1$ these electrons would produce a flux $\nu L_\nu \propto \nu^3$ at $\nu > \nu(r)$, inconsistent with the observed spectrum, and for $\tau_\nu[\nu(r), r] = 1$ these electrons would produce a flux $\nu L_\nu \propto \nu^{4/3}$ at $\nu > \nu(r)$, dominating the emission at $\nu > \nu(r)$ in conflict with the frequency dependence of source size.

We therefore conclude that radiation at different radii r is dominated by electrons with $\nu_c(r) \approx \nu(r)$ and that $\tau_\nu[\nu(r), r] \geq 1$. Next, we argue that the electron energy distribution may be characterized by a single energy or an effective temperature T_e . That is, we show that the energy distribution of electrons cannot be highly non-thermal. Consider, for example, a power-law distribution of electron energies, $dn_e/d\gamma_e \propto \gamma_e^{-p}$. Such a distribution would be consistent with observations provided that $\tau_\nu[\nu(r), r] \approx 1$ (rather than $\tau_\nu[\nu(r), r] \gg 1$), since otherwise the flux emitted by electrons at r would extend beyond $\nu(r)$ as $\nu L_\nu \propto \nu^{7/2}$, exceeding the observed flux. For $\tau_\nu[\nu(r), r] \approx 1$, $\nu L_\nu \propto \nu^{(3-p)/2}$ at $\nu > \nu(r)$, and the value of p is constrained by the ratio between the far-infrared luminosity, $\simeq 3 \times 10^{34}$ erg/s at a frequency $\sim 10^{14}$ Hz [10, 11], and the radio luminosity, $\simeq 5 \times 10^{35}$ erg/s at $\sim 10^{12}$ Hz, to be $p \geq 4.3$. This large power-law index implies that only a small fraction of the total energy can be carried by electrons of energy exceeding that of the electrons dominating the radio emission. Moreover, we will show in § II.3 that the extension of

such a power-law to electron energies much below that of the electrons dominating the radio emission would imply a very large rotation measure, inconsistent with observations [38]. These constraints are satisfied by recent RIAF models [29, 32] which associate only a small fraction of the total electron energy with a power-law component. However, our simple analysis shows that if thermal emission at different frequencies originates at different radii to account for the observed spectrum and size measurements, then there is no need for an ad-hoc non-thermal component.

Since the emission originates from an optically thick plasma, the characteristic temperature (energy) T_e of the electrons dominating the radiation is

$$T_e(r) \approx T_b(r) \approx 7.6(2f_g)^{-1} r_{13}^{1.6\alpha-2} \text{ MeV}. \quad (8)$$

The electron temperature has to satisfy

$$\nu_c(r) = 12 \left(\frac{T_e(r)}{m_e c^2} \right)^2 \times 0.3 \frac{eB(r)}{2\pi m_e c} = \nu(r), \quad (9)$$

where m_e is the electron mass and we used the relation $\langle \gamma_e^2 \rangle = 12[T_e(r)/m_e c^2]^2$ in which angular brackets denote an average over a relativistic Maxwellian of temperature T_e . Based on Eqs. (6) and (5) this requirement implies

$$\left[\frac{T_e(r)}{T_v(r)} \right]^2 B = 27 r_{13}^{2-\alpha} \text{ G}. \quad (10)$$

In deriving this result we have not used the inferred source size but only the fact that it is frequency dependent. Using the size estimate in Eq. (7) and $T_e \approx T_b$, we then get

$$B = 27(2f_g)^2 r_{13}^{4-4.2\alpha} \text{ G}. \quad (11)$$

The $\nu(r) \propto r^{-\alpha}$ scaling of the observed radiation frequency on emission radius implies $T_e \approx T_b = 5\nu_{11}^{-1.6+2/\alpha}$ MeV. In order for the synchrotron model to hold down to ~ 1 GHz, the electrons must remain relativistic, i.e. the condition $5 \times 10^{-2(-1.6+2/\alpha)} > 1$ must hold, implying $1/\alpha \leq 1$ or $\alpha \geq 1$. It therefore appears that the value $1/\alpha \approx 1$ of Shen et al. [27] is preferred over the alternative suggestion for higher values $1/\alpha \approx 1.5 \pm 0.2$ [5].

The results in Eqs. (7), (8) and (11) have several important implications. First, T_e is close to T_v at $r_{13} \sim 1$, and T_e/T_v increases with radius approximately as $r^{1/2}$ for $\beta \sim 1.1$ [39]. This implies that the gas cannot be confined to a thin disk and the flow geometry must be quasi-spherical. Moreover the radio-emitting gas is not likely to be flowing in but rather flowing out since its thermal kinetic energy exceeds the gravitational binding energy beyond a radius of a few tens of Schwarzschild radii ($r_{13} \gtrsim 2$). Our conclusions would only be strengthened if the emitting plasma follows a jet geometry for

which the surface area scales as r^δ with $\delta < 2$ [see the discussion following Eq. (2)].

Finally, we note that the plasma under consideration is collisionless as the Coulomb collision time is much longer than the dynamical time of the gas $2\pi\sqrt{r^3/GM} = 0.9 \times 10^4 r_{13}^{3/2}$ s. However, collective plasma effects should operate [26] since the inverse of the plasma frequency or electron gyro-frequency are much shorter than the dynamical time. We use the term “temperature” in our discussion to characterize the typical electron energy even if the electron distribution function happens to be non-Maxwellian.

II.3. Density constraints: Opacity, Rotation Measure and Circular Polarization

The optical depth to synchrotron self-absorption is

$$\tau[\nu(r), r] = \alpha_\nu r j_\nu = \frac{c^2}{2\nu^2 T_e(r)} r \frac{n_e e^3 B}{m_e c^2} \propto n_e r^{7-3.8\alpha}, \quad (12)$$

giving

$$n_e B = 2.0 \times 10^5 (2f_g)^{-1} \tau(r) r_{13}^{-3-0.4\alpha} \text{ G cm}^{-3}, \quad (13)$$

and

$$n_e = 5.6 \times 10^3 (2f_g)^{-3} \tau(r) r_{13}^{3.8\alpha-7} \text{ cm}^{-3}, \quad (14)$$

For $\alpha \approx 1$ the optical depth increases with radius, $\tau \propto n_e r^3$. In order to ensure that $\tau(r) > 1$, it is sufficient to require that this condition will hold at $r_{13} = 1$, implying $n_e(r_{13} = 1) > 10^3 \text{ cm}^{-3}$.

The relativistic rotation measure of a fluid of electrons with a thermal Lorentz factor γ_e and density n_e threaded by a coherent magnetic field \mathbf{B} , is given by $RRM = 8 \times 10^5 (n_e/\text{cm}^{-3})(B/\text{G})(r/\text{pc})\langle\gamma_e^{-2}\rangle \text{ rad m}^{-2}$ [22]. As long as \mathbf{B} is coherent, we may express this rotation measure in terms of τ as

$$RRM \approx 2.5 \times 10^3 (2f_g) \tau(r) r_{13}^{2-3.6\alpha} \text{ rad m}^{-2} \quad (15)$$

$$= 5 \times 10^5 (2f_g)^4 n_e r_{13}^{9-7.4\alpha} \text{ rad m}^{-2}, \quad (16)$$

where we substituted $\langle\gamma^{-2}\rangle \approx (m_e c^2/T)^2$. For $\alpha \approx 1.1$, the rotation measure scales as $RRM \propto n_e r$ and may be either decreasing or increasing with r . In the latter case, the rotation measure is dominated at all frequencies by the same outermost electron shell, while in the former case it is dominated by electrons near the radius where radiation is emitted (and so it is expected to be larger for higher frequencies or smaller radii). The observed rotation measure of $\sim 6 \times 10^5 \text{ rad/m}^2$ at a frequency of $\sim 2 \times 10^{11} \text{ Hz}$ [Ref. 18, and references therein], implies for a coherent \mathbf{B} -field that

$$n_e \leq 10^6 (2f_g)^{-4} r_{13}^{7.4\alpha-9} \text{ cm}^{-3}. \quad (17)$$

Marrone et al. [18] report measurements at $2.3 \times 10^{11} \text{ Hz}$ and $3.5 \times 10^{11} \text{ Hz}$. While there is an indication that the rotation measure is higher at the higher frequency by a factor of few (see their Table I) the observations at the two frequencies are not simultaneous, and since the source is variable the differences may be due to variability. If the rotation measure differences are real and not due to the temporal variability, Eq. (16) requires

$$n_e(r_{13} = 1) \sim 10^6 (2f_g)^{-4} \text{ cm}^{-3}, \quad (18)$$

with the density decreasing with r at least as steeply as $r^{-9+7.4\alpha}$. For this density (and $f_g \sim 1/2$), the magnetic field and thermal energy densities are comparable at $r_{13} = 1$ and $\tau(r_{13} = 1) \sim 10^2$. A turbulent magnetic field would generate a random walk in the net rotation measure and so the electron density inferred from the *RRM* observations would increase by the square-root of the number of field reversals (coherent \mathbf{B} patches) along the region where the *RRM* originates. The large linear polarization observed at frequencies $\nu > 10^2 \text{ GHz}$ for Sgr A* implies that the inferred magnetic field is not highly tangled in the innermost region. The low level of linear polarization at lower frequencies is consistent with the notion that the emission at different frequencies originates from different radii.

For $\alpha \approx 1$ the electrons become mildly relativistic at $r \sim 10^{15} \text{ cm}$, where the emission is predicted to peak around $\sim 1 \text{ GHz}$. This may account for the circular polarization observed at these low frequencies [3, 4, 24].

Finally, we note that (as mentioned in § II.2) the observed *RRM* excludes a power-law extension of the electron energy distribution, $dn_e/d\gamma_e \propto \gamma_e^{-p}$ with $p \geq 4.3$, down to energies significantly lower than T_e . The contribution of lower energy electrons to the rotation measure is proportional to $n_e/\gamma_e^2 \propto \gamma_e (dn_e/d\gamma_e)/\gamma_e^2 \propto \gamma_e^{-p-1}$. Using Eq. (15) and denoting by γ_m the minimum electron Lorentz factor we have $RRM \approx 2.5 \times 10^3 \tau(T_e/\gamma_m m_e c^2)^{-p-1} \text{ rad/m}^2$, which implies for $p > 4.3$ that the rotation measure would exceed the observed value of $\simeq 5 \times 10^5 \text{ rad/m}^2$ for $\gamma_m m_e c^2/T_e \leq 1/2$.

II.4. Equipartition and Entropy

The equipartition ratio between the magnetic energy density and the thermal energy density of the electrons scales as

$$\frac{B^2/8\pi}{\frac{3}{2} n_e T_e} \propto \frac{r^{10(1-\alpha)}}{n_e}, \quad (19)$$

and the entropy scales as

$$\frac{T_e^3}{n_e} \propto \frac{r^{4.8\alpha-6}}{n_e}. \quad (20)$$

Requiring uniform entropy and equipartition fraction gives $\alpha = 16/14.8 = 1.08$ which is surprisingly within

the range inferred by Shen et al. [27]. This special value yields the scalings $T_e \propto r^{-0.27}$, $n_e \propto r^{-0.82}$, and $B \propto r^{-0.54}$. Substituting these power-law scalings in Eq. (16) implies that the rotation measure RRM is nearly independent of emission radius or observed frequency. This result can be tested by future observations that would monitor the time dependence of RRM at different frequencies [19]. A similar time dependence at different frequencies would imply that the rotation measure is dominated by a common outer shell.

III. COMPARISON WITH EARLIER WORK

The RIAF models generically predict that the radio emission is dominated by thermal electrons near the innermost stable circular orbit (ISCO) in the central region of the accretion disk [31]. The radio spectrum produced in this model by the thermal electrons is inconsistent with the observed spectrum, which is well described by the power-law form in Eq. (1). A power-law electron component is therefore added to the thermal RIAF component in an ad-hoc manner, where the spectral index and normalization of the power-law component are tailored to match the low frequency radio data [29, 32]. We have pointed out in § II.2 that the size measurements indicate that the source size is frequency dependent, implying that the radiation is dominated at different frequencies by electrons at different locations. This in turn suggests that the observed spectrum reflects the spatial dependence of electron temperature rather than the energy distribution of the electrons at a single radius.

Since the emission of radiation in RIAF models is dominated by the innermost region of the disk, at $r \sim 3R_s = 3.6 \times 10^{12}$ cm, the observed size is dominated in these models by foreground interstellar scattering at all frequencies. The addition of a power-law electron component to these models increases slightly the intrinsic source size [33], but does not change the requirement that the measured source size will be dominated at all frequencies by interstellar medium scattering. These results appear to be at odds with the latest size measurements which indicate that the intrinsic size is resolved well beyond the expected level of interstellar image broadening at $\lambda \leq 3.5$ mm [14] and that the intrinsic size is smaller at higher frequencies.

As mentioned in the Introduction, existing size measurements are subject to large uncertainties. While our best-fit profiles disfavor existing models, such models cannot be ruled out based on current data. Future, more accurate, measurements will allow us to draw more decisive conclusions. Our current analysis underlines the importance of future improvements in the size measurements, and provides a methodology for interpreting future results.

IV. SUMMARY

We have shown in § II.2 that measurements of the spectrum and of the wavelength-dependent size of the radio emission from Sgr A* indicate that this emission is dominated by optically-thick quasi-thermal plasma, and that the observed spectrum reflects the spatial dependence of the electron temperature (rather than the energy distribution of electrons at some particular radius). We have derived the electron temperature and magnetic field profiles [Eqs. (8) and (11)], and found that the electron temperature increases above the virial temperature beyond a distance of a few tens of Schwarzschild radii from the black hole. The observed rotation measure was then used to constrain the density profile [Eqs. (17) and (18)]. The low density inferred for the gas near Sgr A* could in principle be accounted for by winds from the innermost S-stars [16]. Although we have not proposed a dynamical model for the plasma, we have pointed out in § II.4 that observations are consistent with an isentropic gas profile and equipartition magnetic field.

Our results imply that the radio emitting gas cannot be confined to a thin disk and the flow geometry must be geometrically thick. Moreover, the radio-emitting gas is not likely to be inflowing but rather outflowing, since its thermal kinetic energy exceeds the gravitational binding energy beyond a radius of a few tens of Schwarzschild radii [$r_{13} \gtrsim 2$, see Table I and Eq. (7)]. There may also be a colder accreting component that is sub-dominant in terms of its synchrotron emission. Such a component would likely be confined to a thinner disk geometry that would have only a limited effect on the rotation measure of the radiation emitted by the hot outflowing atmosphere above it. (However, if the cold component is optically-thick then it would make the image of Sgr A* asymmetric at a level that would depend on the inclination of the disk. The resulting frequency dependence of the image centroid location could be constrained by observations.) An electron temperature profile which does not decline with increasing radius as fast as the virial temperature does, would be consistent with an adiabatic outflow in which the electrons are hotter than the protons because their relativistic temperature declines with decreasing density as $T \propto n^{\Gamma-1}$ with an adiabatic index ($\Gamma = 4/3$) that is smaller than that of the protons ($5/3$). Heat conduction could also help to flatten the electron temperature profile [20].

The large uncertainty in the inferred source size, reflected by the large uncertainty in the index $\alpha = 1 \pm 0.3$ of the relation $r \propto \nu^\alpha$, translates to a large uncertainty in the temperature and magnetic field profiles, as implied by Eqs. (11) and (8). Our preliminary conclusions from existing data differ from current theoretical models [29], although not at a statistically robust level. These potential discrepancies provide added incentive to obtain

better data through future observations.

Finally, we note that the uncertainty in the determination of the density profiles is related not only to uncertainties in the source size measurements, but also to the lack of simultaneous multi-frequency measurements of the rotation measure (§ II.3). An accurate determination of the density profile would require therefore not only accurate size measurements, but also simultaneous multi-frequency measurements of the rotation measure. Ultimately, direct imaging of Sgr A* with a Very Large Baseline Array at sub-mm wavelengths [6, 9, 28] would resolve the accretion flow near the black hole ISCO and unravel unambiguously the properties of the emitting gas there.

Acknowledgments We thank Avery Broderick, Dan Marrone, and an anonymous referee for useful comments on the manuscript. A.L. thanks the Weizmann Institute for its kind hospitality when this work was conducted. This work was supported in part by ISF and Minerva grants (E. W.) and the BSF foundation (A. L.).

[1] Agol, E. 2000, *ApJ Lett.*, 538, L121

[2] Blandford, R. D., & Begelman, M. C. 1999, *MNRAS*, 303, L1

[3] Bower, G. C., Falcke, H., & Backer, D. C. 1999, *ApJ Lett.*, 523, L29

[4] Bower, G. C. 2003, *Astrophys. & Space Sci.*, 288, 69

[5] Bower, G. C. 2006, *Journal of Physics Conference Series*, 54, 370; Bower, G. C., Goss, W. M., Falcke, H., Backer, D. C., & Lithwick, Y. 2006, *ApJ Lett.*, 648, L127

[6] Broderick, A. E., & Loeb, A. 2006, *Journal of Physics Conference Series*, 54, 448 [astro-ph/0607279]; 2006, *MNRAS*, 367, 905

[7] Eckart, A., Genzel, R., & Schödel, R. 2004, *Progress of Theoretical Physics Supplement*, 155, 159

[8] Falcke, H., Goss, W. M., Matsuo, H., Teuben, P., Zhao, J.-H., & Zylka, R. 1998, *ApJ*, 499, 731

[9] Falcke, H., Melia, F., & Agol, E. 2000, *ApJ Lett.*, 528, L13

[10] Genzel, R., Schödel, R., Ott, T., Eckart, A., Alexander, T., Lacombe, F., Rouan, D., & Aschenbach, B. 2003, *Nature (London)*, 425, 934

[11] Ghez, A. M., et al. 2004, *ApJ Lett.*, 601, L159

[12] Goldston, J. E., Quataert, E., & Igumenshchev, I. V. 2005, *ApJ*, 621, 785

[13] Krichbaum, T. P., et al. 1998, *A& A*, 335, L106

[14] Krichbaum, T. P., Graham, D. A., Bremer, M., Alef, W., Witzel, A., Zensus, J. A., & Eckart, A. 2006, *Journal of Physics Conference Series*, 54, 328 [astro-ph/0607072]

[15] Liu, S., & Melia, F. 2003, *Astronomische Nachrichten Supplement*, 324, 475

[16] Loeb, A. 2004, *MNRAS*, 350, 725

[17] Macquart, J.-P., Bower, G. C., Wright, M. C. H., Backer, D. C., & Falcke, H. 2006, *ApJ Lett.*, 646, L111

[18] Marrone, D. P., Moran, J. M., Zhao, J.-H., & Rao, R. 2007, *ApJ Lett.*, 654, L57

[19] Marrone, D. P. 2007, private communication

[20] Gruzinov, A. 2008, preprint astro-ph/9809265; Tanaka, T., & Menou, K. 2006, *ApJ*, 649, 345

[21] Narayan, R., Mahadevan, R., & Quataert, E. 1998, *Theory of Black Hole Accretion Disks*, 148; Quataert, E., Narayan, R., & Reid, M. J. 1999, *ApJ Lett.*, 517, L101

[22] Quataert, E., & Gruzinov, A. 2000, *ApJ*, 545, 842

[23] Quataert, E., & Gruzinov, A. 2000, *ApJ*, 539, 809; Narayan, R., Igumenshchev, I. V., & Abramowicz, M. A. 2000, *ApJ*, 539, 798

[24] Sault, R. J., & Macquart, J.-P. 1999, *ApJ Lett.*, 526, L85

[25] Serabyn, E., Carlstrom, J., Lay, O., Lis, D. C., Hunter, T. R., & Lacy, J. H. 1997, *ApJ Lett.*, 490, L77

[26] Sharma, P., Hammett, G. W., Quataert, E., & Stone, J. M. 2006, *ApJ*, 637, 952

[27] Shen, Z.-Q., Lo, K. Y., Liang, M.-C., Ho, P. T. P., & Zhao, J.-H. 2005, *Nature (London)*, 438, 62

[28] Shen, Z.-Q. 2005, *Journal of Korean Astronomical Society*, 38, 261

[29] Yuan, F. 2006, *Journal of Physics Conference Series*, 54, 427 [astro-ph/0607123]

[30] Yuan, F., Markoff, S., & Falcke, H. 2002, *A& A*, 383, 854; Falcke, H. & Markoff, S. 2000, *Astron. & Astrophys.*, 362, 113

[31] Yuan, F., Quataert, E., & Narayan, R. 2003, *ApJ*, 598, 301

[32] Yuan, F., Quataert, E., & Narayan, R. 2004, *ApJ*, 606, 894

[33] Yuan, F., Shen, Z.-Q., & Huang, L. 2006, *ApJ Lett.*, 642, L45

[34] Zhao, J.-H., Young, K. H., Herrnstein, R. M., Ho, P. T. P., Tsutsumi, T., Lo, K. Y., Goss, W. M., & Bower, G. C. 2003, *ApJ Lett.*, 586, L29

[35] Zylka, R., Mezger, P. G., Ward-Thompson, D., Duschl, W. J., & Lesch, H. 1995, *A& A*, 297, 83

[36] For an optically thick source with a top-hat intensity distribution, the full-width at half-maximum (FWHM) of a Gaussian which contains the same flux fraction as the top-hat within the FWHM size is $\sqrt{2/\pi} \int_0^{\sqrt{2\log 2}} dx \exp(-x^2/2) = 0.76$ times the source diameter. We use this result when interpreting the values quoted by Krichbaum et al. [14] for the geometric mean of FWHM of the major and minor axes of the image of Sgr A*.

[37] Throughout the paper, we set Boltzmann's constant k_B to unity and express temperatures in energy units.

[38] One may postulate, of course, a power-law distribution with $p < 4.3$, which cuts off just above the energy of the electrons we observe (so as to avoid overproducing the 10^{14} Hz flux). However, such a cut-off would be physically unnatural.

[39] Note that for $\alpha = 1/1.6 = 0.625$, which might still be consistent with observations [5], $T_e/T_v = \text{const}$, but then $B^2 \propto r^{2.75}$ which is physically implausible.